Giner, Eugenio, … et al. (2015) Estimation of the reinforcement factor ξ for calculating the transverse stiffness E2 with the Halpin-Tsai equations using the finite element method. *Composite Structures*, v. 124, pp.: 402-408.

DOI: https://doi.org/10.1016/j.compstruct.2015.01.008

Estimation of the reinforcement factor ξ for calculating E_2 with the Halpin-Tsai equations using the finite element method

Eugenio Giner[a,*], Ana Vercher[a], Miguel Marco[b], Camila Arango[a]

[a] *Centro de Investigación en Ingeniería Mecánica - CIIM, Dept. of Mechanical Engineering and Materials, Universitat Politècnica de València, Camino de Vera s/n, 46022 Valencia, Spain.*
[b] *Dept. of Mechanical Engineering Universidad Carlos III de Madrid, Av. de la Universidad 30, 28911 Leganés, Madrid, Spain.*

Abstract

In this work, an estimation of the reinforcement factor ξ of the Halpin-Tsai equations used to calculate the transverse stiffness E_2 is provided. A better estimation of the value $\xi = 2$ originally proposed by Halpin and Tsai is given through a set of finite element analyses that consider randomly distributed unidirectional fibers for different volume fractions. The analysis overcomes the original hypothesis of a square array distribution of fibers in the transverse plane. It is concluded that a value of $\xi = 1.5$ is a better estimation for the usual volume fractions found in practice for a unidirectional lamina of fiber reinforced composites.

Keywords: Reinforcement factor, transverse stiffness, unidirectional lamina, finite element analysis.

*Corresponding author. Tel.: +34-96-3877007 ext. 76218; fax: +34-96-3877629.
Email address: eginerm@mcm.upv.es (Eugenio Giner)

1. Introduction

The Halpin-Tsai equations [1] are widely used to calculate elastic properties of different configurations of composite materials. Among these properties, one of the most relevant is the transverse stiffness E_2 of a unidirectional lamina with oriented continuous fibers. It is well known that approaches based on a strength of materials analysis underestimate the true value of E_2, leading to a lower bound of E_2 (Reuss boundary) [2]. In the past a large number of models have been proposed in the literature to obtain more accurate estimations of E_2 and other elastic constants, many based in formal approaches of the theory of elasticity (see the excellent reviews in [1, 2]). These models account for the matrix-dominant effect on the homogenized value E_2 for a lamina, such as the Ekvall model [2] that considers the triaxial stress state in the matrix due to fiber restraint.

It has been extensively verified that the Halpin-Tsai (H-T) equations are a good practical way for calculating E_2, using the originally proposed value of the reinforcement factor $\xi = 2$. The wide application of the H-T equations heavily relies on their simplicity, which is desirable for design purposes. The reinforcement factor ξ varies with the geometry of the reinforcement, its distribution and the volume fraction. Originally, the value of ξ for oriented continuous fibers was derived by Halpin and Tsai from correlation with analytical solutions that assume an idealized geometrical distribution or pattern (e.g. Adams and Doner solution for a square array of fibers solved by a finite-difference scheme). Some approximate equations for ξ are also given in the literature to modify the value of ξ for high volume fractions, as recalled in Section 2.

A question arises about the influence of a random distribution of the reinforcement in the transverse plane 2-3, which is much more realistic than a mere square arrangement. Since ξ takes into account the effect of the geometry and distribution of the reinforcement, it is expected that this random distribution may have a non negligible effect. In this work, we carry out a series of parametric finite element analysis with different random distributions of fibers of circular cross section to quantify the influence of the random distribution. Several volume fractions are considered and the diameter of the fiber cross section is also varied randomly between the usual ranges.

An inverse analysis enables the estimation of ξ for different volume fractions, leading to the conclusion that a more convenient value of ξ is about 1.5 for typical volume fractions instead of the typical value of 2.0 derived from an idealized square arrangement usually found in the literature. An important deviation is also found for low and high volume fractions. Some approximate equations are also provided for these ranges of volume fraction.

2. Calculation of E_2 using the Halpin-Tsai equations

The H-T equations were developed in the late sixties [6] with the aim of providing a simple but an effective way of calculating the elastic properties of a fiber reinforced lamina, since previous developments led to complicated equations difficult to use. Halpin and Tsai developed an interpolation procedure attempting to gather the main results of those micromechanics analyses. The success of the H-T equations is based both on their simplicity and on the generalization of previous micromechanics results cumbersome to use, together with the relatively accurate estimations provided for usual volume

fractions. Thus, these equations are often termed as semiempirical [4], as they are based on mechanical fundamentals.

The H-T equations can be found in many books on mechanical behaviour of composite materials [1–4]. The H-T equation for the transverse modulus E_2 is:

$$\frac{E_2}{E_\mathrm{m}} = \frac{1 + \xi\eta V_\mathrm{f}}{1 - \eta V_\mathrm{f}} \tag{1}$$

where

$$\eta = \frac{E_\mathrm{f}/E_\mathrm{m} - 1}{E_\mathrm{f}/E_\mathrm{m} + \xi} \tag{2}$$

being E_f, E_m the fiber and matrix modulus, respectively, and ξ is the reinforcement parameter, which is the parameter estimated in this work. Analogous equations are formulated for G_{12} and ν_{23} [1–4]. For the longitudinal modulus E_1 and ν_{12} the well-known rule of mixtures holds [1]. The only difficulty in using the Halpin-Tsai equations seems to be the determination of a suitable value for ξ. Halpin and Tsai proposed a value of $\xi = 2$ for calculation of E_2 and $\xi = 1$ for calculation of G_{12} after obtaining an excellent agreement with Adams and Doner's results for circular fibers in a square array at a fiber volume fraction of 0.55.

The reinforcement parameter ξ depends on the fiber geometry, fiber distribution and loading conditions. It can be shown [2] that when $\xi = 0$ Eq. (1) reduces to the lower bound for E_2 given by a strength of materials approach, whereas when $\xi = \infty$ the rule of mixtures for E_1 is recovered (the theoretical upper bound for E_2). Thus, it is said that ξ is a measure of the degree of matrix reinforcement by the fibers.

For high V_f, the constant value of $\xi = 2$ does not provide good results for E_2 and modifying equations have been proposed. For example, for $V_\mathrm{f} \geq 0.65$,

Hewitt and de Malherbe [7] suggested an equation for ξ that provides better agreement with analytical results. For the case of E_2, this equation is [1]:

$$\xi(V_\mathrm{f}) = 2 + 40V_\mathrm{f}^{10} \tag{3}$$

Spencer [8] provided an equation that is a modification of the H-T equations for E_2 and G_{12} for a wide range of V_f and for three repetitive regular packing arrays: square, triangular[1] and hexagonal. His proposal includes an adjusted parameter that modifies the square array solution for very high V_f to approach an hexagonal packing behaviour.

The H-T equations are also applicable to other reinforcement geometries, such as ribbon or particulate reinforcements. In [1], a comprehensive summary of ξ values for other reinforcement geometries is given.

Since it is accepted that the values of ξ are obtained by comparing (1) with exact elasticity solutions by fitting procedures [1, 2], the aim of this work is to estimate the value of ξ with the elastic solutions provided by finite element analyses. Given that our analyses take into account the geometric effect of the random distribution of fibers in the plane 2-3 and also the variations in fiber diameter that are found in practice, it is expected that the estimations for ξ will be more accurate than the current available values.

3. Calculation of E_2 and ξ using finite element models

In order to estimate a better value for ξ to calculate E_2, numerical models of the unidirectional fiber reinforced lamina have been realized by means of

[1]In [8], the triangular array corresponds to what is often called hexagonal array, like in this work. In [8], the so-called hexagonal array is a variation of the triangular array.

the finite element method. We consider a fiber-oriented coordinate system $(1, 2, 3)$, being the 1-axis aligned with the fiber direction. The cross section analyzed in this work belongs to the $2-3$ plane, as shown in Fig. 1. We assume a plane strain condition for the stress state at a given cross section, due to the longitudinal stiffness provided by the fibers.

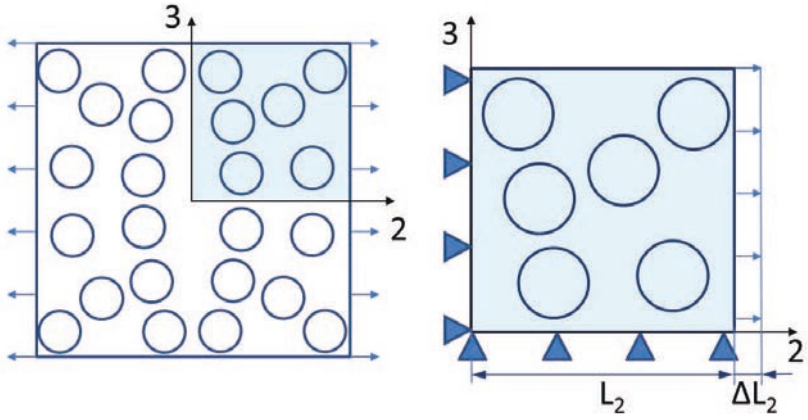

Figure 1: Cross section in plane $2-3$ and sketch of the domain analyzed numerically. A uniaxial uniform strain $\varepsilon_2 = \Delta L_2/L_2$ is applied. Symmetry boundary conditions are considered.

The domain is subjected to uniaxial uniform strain in direction 2 by enforcing a given displacement for the right boundary, i.e. $\varepsilon_2 = \Delta L_2/L_2$, see Fig.1. Symmetry boundary conditions are applied, which are equivalent to consider a domain that is four times the domain actually analyzed. Three arrangements of fibers have been considered: square array, hexagonal array and random distribution, as described in Section 4.

3.1. Calculation of E_2

By assuming a linear elastic behavior, the generalized Hooke's law in terms of the compliance matrix $\mathbf{S}$ for an orthotropic lamina is:

$$\begin{Bmatrix} \varepsilon_1 \\ \varepsilon_2 \\ \varepsilon_3 \\ \gamma_{23} \\ \gamma_{31} \\ \gamma_{12} \end{Bmatrix} = \begin{pmatrix} S_{11} & S_{12} & S_{13} & 0 & 0 & 0 \\ S_{12} & S_{22} & S_{23} & 0 & 0 & 0 \\ S_{13} & S_{23} & S_{33} & 0 & 0 & 0 \\ 0 & 0 & 0 & S_{44} & 0 & 0 \\ 0 & 0 & 0 & 0 & S_{55} & 0 \\ 0 & 0 & 0 & 0 & 0 & S_{66} \end{pmatrix} \begin{Bmatrix} \sigma_1 \\ \sigma_2 \\ \sigma_3 \\ \tau_{23} \\ \tau_{31} \\ \tau_{12} \end{Bmatrix} \tag{4}$$

As only a uniform strain in direction 2 is applied, the global equilibrium implies that $\sigma_3 = 0$ and $\tau_{23} = 0$ due to the symmetry of the solution. Additionally, the plane strain condition implies that $\varepsilon_1 = 0$, $\gamma_{31} = 0$ and $\gamma_{12} = 0$. Therefore, the strain-stress relationship (4) can be reduced to

$$\begin{Bmatrix} 0 \\ \varepsilon_2 \\ \varepsilon_3 \end{Bmatrix} = \begin{pmatrix} S_{11} & S_{12} & S_{13} \\ S_{12} & S_{22} & S_{23} \\ S_{13} & S_{23} & S_{33} \end{pmatrix} \begin{Bmatrix} \sigma_1 \\ \sigma_2 \\ 0 \end{Bmatrix} \tag{5}$$

From the first equation of (5), it can be written:

$$\sigma_1 = -\frac{S_{12}}{S_{11}}\sigma_2 \tag{6}$$

Recalling the symmetry of the compliance matrix $\mathbf{S}$ and expressing its components in terms of engineering elastic constants:

$$\sigma_1 = -\frac{-\nu_{12}/E_1}{1/E_1}\sigma_2 = \nu_{12}\sigma_2 \tag{7}$$

and substituting this result in the second equation of (5):

$$\varepsilon_2 = \left(\frac{1}{E_2} - \frac{\nu_{12}^2}{E_1}\right)\sigma_2 \tag{8}$$

From this equation, an explicit expression for E_2 under a plane strain assumption can be obtained:

$$E_2 = \frac{E_1 \sigma_2}{E_1 \varepsilon_2 + \nu_{12}^2 \sigma_2} \tag{9}$$

Equation (9) is used to estimate E_2 from the numerical analyses of this work, since ε_2 is the applied uniform strain $\Delta L_2/L_2$ and σ_2 is computed simply as the summation of the reaction forces at the right boundary divided by the net section at that boundary (we have assumed unit thickness). On the other hand, E_1 and ν_{12} are obtained from the constituent properties through the rule of mixtures, which holds for E_1 and ν_{12} as part of the H-T equations [1]:

$$E_1 = E_\mathrm{f} V_\mathrm{f} + E_\mathrm{m}(1 - V_\mathrm{f}) \tag{10}$$

$$\nu_{12} = \nu_\mathrm{f} V_\mathrm{f} + \nu_\mathrm{m}(1 - V_\mathrm{f}) \tag{11}$$

3.2. Calculation of ξ

For the computation of ξ, the value of E_2 is first calculated through (9) and introduced in equation (1). Then, an iterative procedure is used to solve simultaneously (1) and (2) for ξ and η until the solution converges.

4. Numerical analyses for square and hexagonal arrays. Results

The analyses have been performed with the finite element commercial code Ansys$^{\mathrm{TM}}$. 2D models have been meshed with quadratic triangular elements (see Fig. 2) and the fiber cross-section is circular for all cases. Both matrix and fibers have been considered isotropic and perfectly connected through their interfaces. In order to perform the analyses and compute E_2 and ξ, some material properties have been fixed as follows: $E_\mathrm{f} = 250$ GPa,

$\nu_f = 0.30$, $E_m = 5$ GPa, $\nu_m = 0.38$, which correspond to typical values for carbon fiber and epoxi resin, respectively. However, the material properties are not relevant, since ξ depends on the reinforcement geometry and distribution, but not on the material properties. This has been verified by making a sensitivity analysis to the material properties (changed to typical glass fiber and polyester resin composite with $E_f = 72$ GPa, $\nu_f = 0.25$, $E_m = 3.5$ GPa, $\nu_m = 0.37$). As expected, the obtained estimations for ξ are virtually coincident.

4.1. 2D square arrays

The first set of analyses are performed for a square array of fibers. The aim of this section is to verify that the prediction of our numerical model and calculation procedure is in agreement with the H-T equation using the customary value of $\xi = 2$, fitted originally for the Adams and Doner's analytical solution for a square array. A total of 14 analyses have been carried out for different fiber volume fractions, starting from $V_f = 0.05$ to $V_f = 0.7$ (close to the maximum theoretical value for a square array) at increments of 0.05. Fig. 2, left, shows the FE model for the case $V_f = 0.4$. The geometrical models have been automatically generated by dedicated macros. In this section, all fibers are assumed to have the same diameter: 7.2 μm.

Results are shown in Fig. 3. The solid curve denoted as H-T refers in fact to the ξ estimation provided by Eq. (3) given by Hewitt and de Malherbe, which reduces to $\xi = 2$ for a wide range of V_f. The estimation of ξ using the square array numerical models leads to slightly lower values of ξ specially for V_f in the range $[0.1, 0.5]$. Note the good agreement between the square array numerical solution and the H-T and Hewitt and de Malherbe solution in the

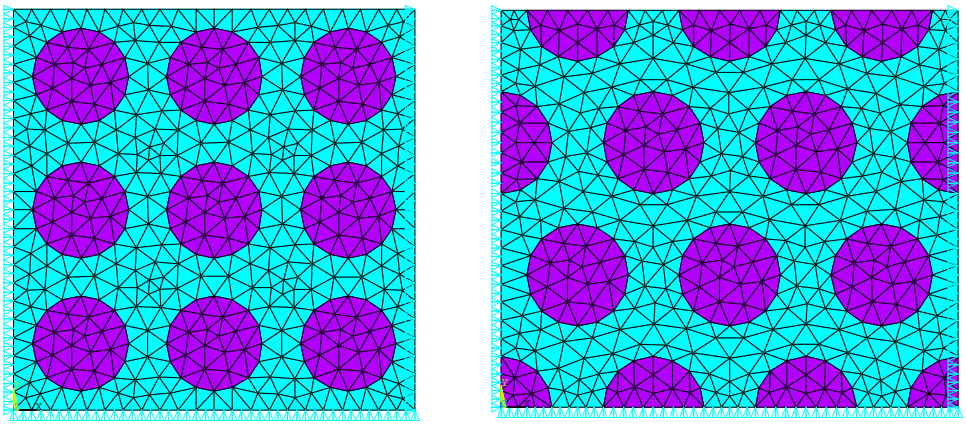

Figure 2: FE meshes for square and hexagonal arrays, case $V_{\mathrm{f}} = 0.4$. Displacement boundary conditions are shown.

range $[0.50, 0.55]$, where it is reported that the H-T solution matches very well the Adams and Doner's solution for a square array [1, 2].

A more thorough validation of our numerical procedure is provided in Fig. 4, where the numerical estimations of the normalized value E_2/E_{m} for square arrays with different V_{f} are correlated with the analytical curves provided by Adams and Doner's [1, 2]. Their curves were computed for different constituent properties (different ratios $E_{\mathrm{f}}/E_{\mathrm{m}}$). We computed five different constituent property ratios combined with six different V_{f}. In Fig. 4, the estimations of E_2/E_{m} are superimposed on the original Adams and Doner's curves, yielding a good agreement. There are only differences for very high volume fractions ($V_{\mathrm{f}} > 0.7$). We remark that, for $V_{\mathrm{f}} > 0.7$, the square array is very close to the theoretical maximum packing value ($V_{\mathrm{f,max\ sq}} = 0.785$ [3]). The numerical models are not accurate in this situation, as we have verified that there is a high strain concentration localized at the right boundary,

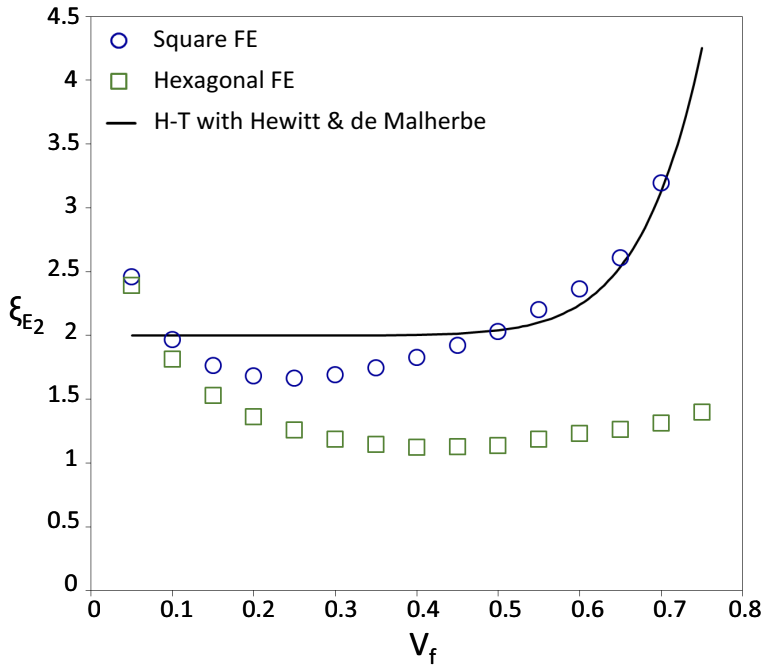

Figure 3: Comparison of ξ values given by the Halpin-Tsai value ($\xi = 2$) modified with the Hewitt and de Malherbe approximation, Eq. 3, and the numerical estimations with square and hexagonal arrays.

where the forced displacement is prescribed. Therefore, boundary effects of our numerical model start affecting the results for such high volume fractions. We note in passing that the situation of a perfect square array fiber distribution with $V_\mathrm{f} > 0.7$ is unrealistic in practice. For usual volume fractions $V_\mathrm{f} < 0.7$, we conclude from this study that the numerical model conveniently reproduces the expected solution when a square array of fibers is assumed.

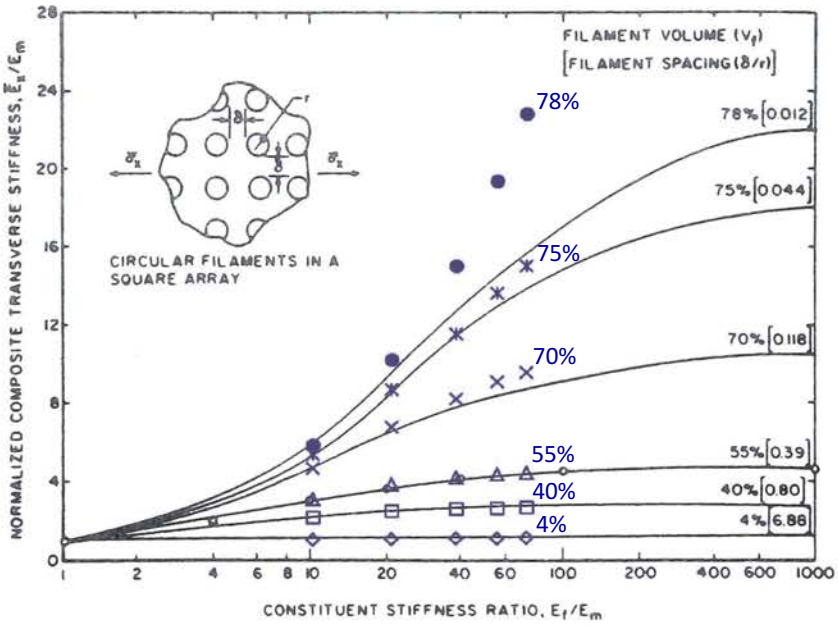

Figure 4: Square array FE estimations of E_2 and comparison to Adams and Doner's analytical solutions.

4.2. 2D hexagonal arrays

Models with an hexagonal array have been also analyzed, see Fig. 2 right. It is worth noting that the estimation of ξ when an hexagonal array is considered (see Fig. 3) yields values that are remarkably lower than the ones provided by Eq. (3). As a true fiber distribution is neither a square nor hexagonal array, this motivated us to perform analyses with random distributions, as shown in Section 5. In next subsections we first analyze the sensitivity of the 2D model to several aspects.

4.3. Sensitivity of the 2D model

Several sensitivity analyses have been carried out to verify that the 2D models are sufficiently accurate. As detailed next, we have verified that the proposed procedure and the 2D models yield accurate enough results.

4.3.1. Sensitivity to domain size

In our analyses, the domain size must be sufficiently large to minimize the end-border effects and, thus, characterize the proper elastic response of a lamina in the transverse direction. Fig. 5 shows both the standard domain size used in this work (above) and the larger domain sizes used to verify the insensitivity of the results to the domain size (below). The strain concentration in the ε_2 field is plotted qualitatively to appreciate the slight differences near the boundaries that rapidly disappear inside the domain.

Fig. 6 shows the estimations of ξ for three different volume fractions considering the standard and large domain sizes and both the square and hexagonal arrays. It can be seen that the difference is negligible, so we concluded that the standard domain size is sufficient to ignore the boundary effects.

4.3.2. Sensitivity to 3D effects

Full 3D models with square and hexagonal arrays have been also realized to avoid the 2D assumption of plane strain. Fig. 7 shows these domains with the qualitative distribution of ε_2 for $V_\mathrm{f} = 0.4$. In this 3D case, the procedure for computing ξ does not need the derivation given in Section 3.1 and Eq. 9 for a plane strain condition. E_2 is simply calculated as σ_2/ε_2, i.e. the average transverse stress computed from the reaction forces is divided by

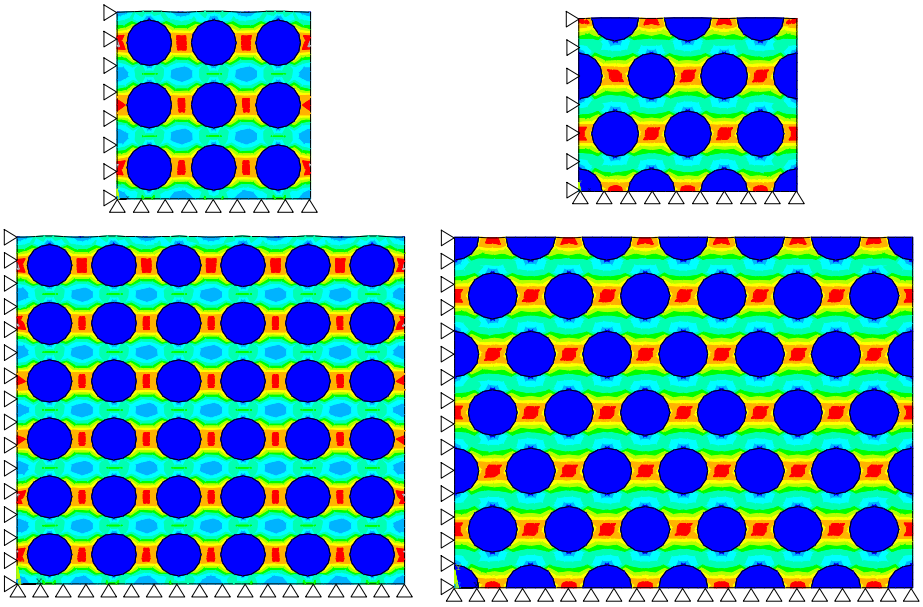

Figure 5: Above: standard domains for the square and hexagonal arrays used in this work. Below: large domains to verify the sensitivity to the domain size. All models for $V_\mathrm{f} = 0.4$. The field represented is ε_2, showing qualitatively the strain concentration in the matrix produced by the forced displacement of Fig. 1.

the prescribed transverse strain, $\varepsilon_2 = \Delta L_2/L_2$.

The results shown in Fig. 8 show that the differences between the 2D and 3D estimations for ξ are very small, confirming that the 2D models are accurate enough, thus simplifying the model generation and reducing the computational cost.

4.3.3. Sensitivity to material properties

As explained in Section 1, the reinforcement factor ξ is a geometric parameter that takes into account the shape and distribution of the reinforcement and, therefore, it is material independent. We verify numerically this fact

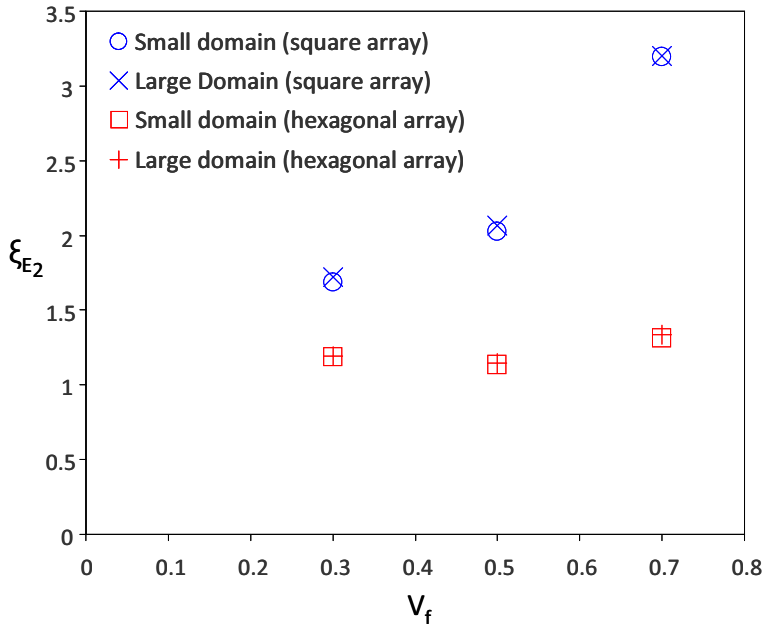

Figure 6: Sensitivity analysis to the domain sizes shown in Fig. 5 for three V_{f} (square and hexagonal arrays).

also in this subsection. Three pairs of constituent properties have been studied: $E_{\mathrm{f}} = 72$ GPa and $E_{\mathrm{m}} = 3.5$ GPa; $E_{\mathrm{f}} = 72$ GPa and $E_{\mathrm{m}} = 2$ GPa; $E_{\mathrm{f}} = 250$ GPa and $E_{\mathrm{m}} = 5$ GPa. These values can be considered typical of glass and carbon fibers, polyester and epoxi resins. The analyses have been carried out with the 2D standard domains for both square and hexagonal arrays for three different V_{f}.

Fig. 9 shows that all the ξ estimations are independent of the material properties considered, except for the case square array and $V_{\mathrm{f}} = 0.7$, for which slight differences are observed. This is due to the high V_{f} value, which is close to the theoretical maximum packing value for a square array ($V_{\mathrm{f,max\ sq}} =$

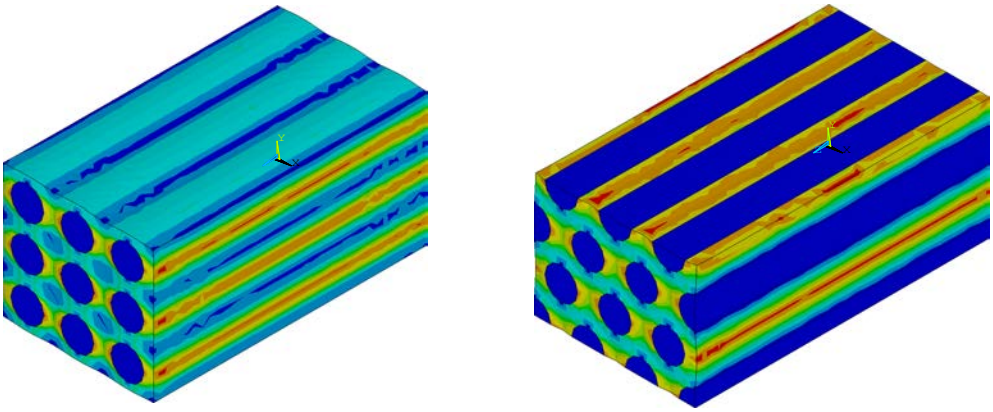

Figure 7: 3D domains to verify the insensitivity to the 2D plane strain assumption. Models for $V_f = 0.4$. The field represented is ε_2, showing qualitatively the strain concentration in the matrix produced by the forced displacement of Fig. 1.

0.785 [3]). As commented above, for high V_f we have verified that the 2D standard domain shows a high strain concentration localized at the right boundary, where the forced displacement is prescribed. Therefore, the slight material dependency shown for a square array and $V_f = 0.7$ is due to the limitations of the numerical model. This is in line with the results presented in the comparison with the Adams and Doner's solution of Fig. 4 for different constituent properties ratios and high V_f. Hence, we can conclude that the estimation of the reinforcement factor ξ is material independent as expected.

5. Numerical analyses for random distribution. Results

The same procedure has been followed with models generated by a random distribution. The geometrical models have been generated by routines developed in Matlab. Fig. 10 shows three of the geometrical models for the

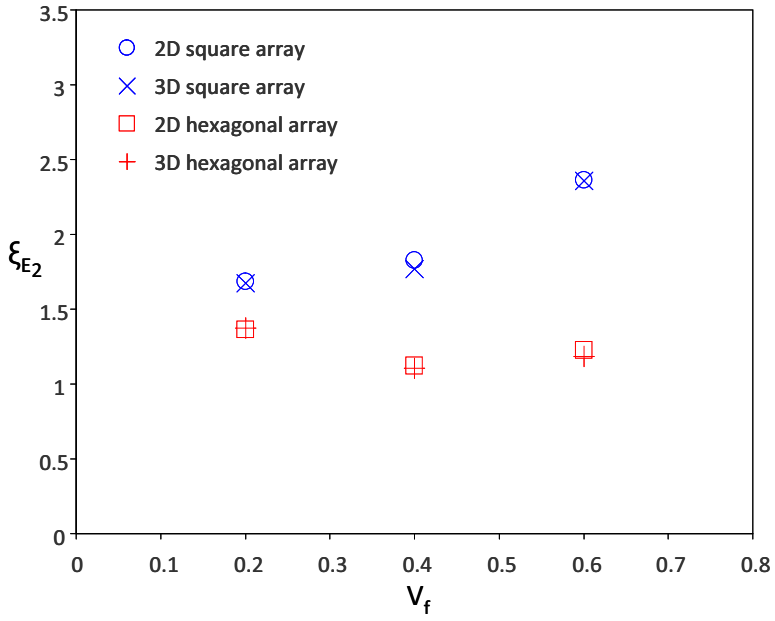

Figure 8: Sensitivity analysis to 3D effects using the 3D models shown in Fig. 7 for three V_{f} (square and hexagonal arrays).

.

cases $V_{\mathrm{f}} = 0.2$, 0.4 and 0.6. Note that eventual contacting fibers are allowed, as actually expected.

In addition, we have also considered the random variation of the fiber diameter. Although small, this can have a certain amount of influence, since ξ is a parameter that depends on the geometry of the reinforcement and its distribution. From cross section micrographs available in the literature (e.g. [3]), we have measured the distribution of diameters and generated geometrical models that account for the diameter variation. In these random-distributed models, the previous diameter of 7.2 μm has been varied in the range $[6.7, 7.7]\,\mu$m, as can be observed in Fig. 10. Note also that the domain

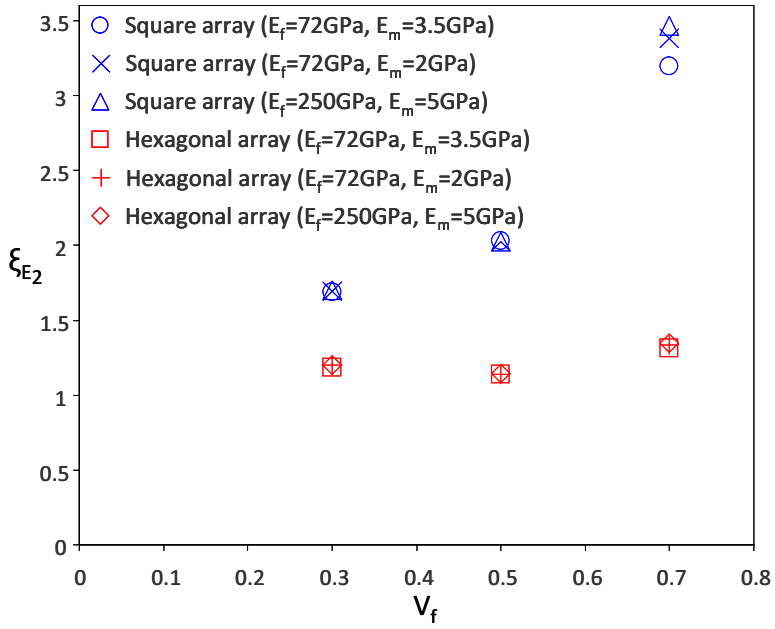

Figure 9: Sensitivity analysis to the constituent material properties for three V_{f} (square and hexagonal arrays).

size is adjusted for each volume fraction so as to respect the fiber diameters, i.e. the domains in Fig. 10 are not to scale.

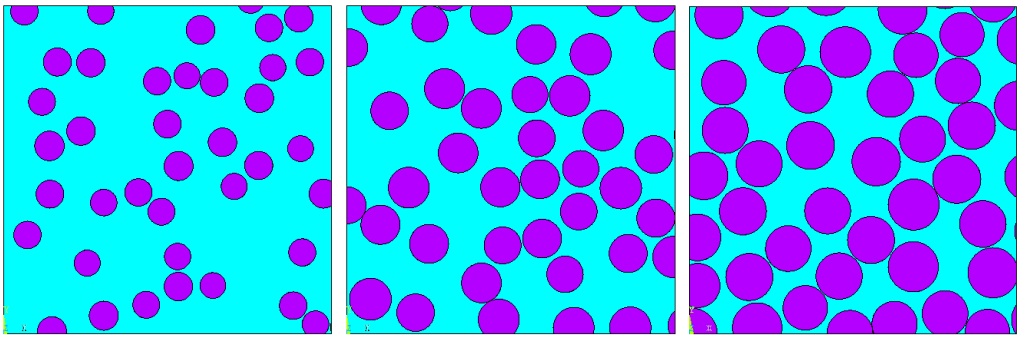

Figure 10: Geometrical models. Random distributions for the cases $V_{\mathrm{f}} = 0.2$, 0.4 and 0.6.

As the distribution of the fibers and diameters is now random, we have generated three models around each volume fraction in the range $[0.05, 0.6]$, at increments of 0.05. Note that it has not been possible to generate a random geometrical model with $V_{\mathrm{f}} > 0.65$ due to fiber packing issues, as may happen in practice. Note also that for each random model, the actual V_{f} has been measured after the model is generated and this leads to a slight scatter in the values of V_{f} shown in Fig. 11. A total number of 39 random models have been analyzed.

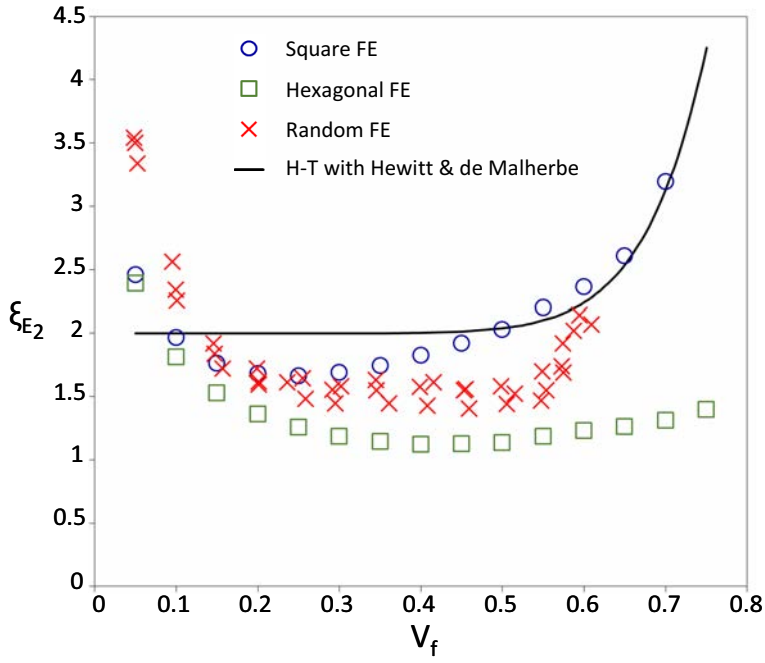

Figure 11: Comparison of ξ values given by the Halpin-Tsai value ($\xi = 2$) modified with the Hewitt and de Malherbe approximation, Eq. (3), and the numerical estimations with square array, hexagonal array and random distribution.

The results in Fig. 11 show that the estimated values of ξ lie below the

ones provided by the Hewitt and de Malherbe equation (3) and between the values obtained for square and hexagonal arrays. As shown in Fig. 11, a value of $\xi = 1.5$ seems to be more appropriate for volume fraction in the range $[0.25, 0.55]$ than the customary value $\xi = 2$. For a wider range of volume fractions, the following analytical expressions have been fitted to the ξ estimations for random arrays, see Fig. 12:

$$\xi(V_\mathrm{f}) = \begin{cases} 4.924 - 35.888\,V_\mathrm{f} + 125.118\,V_\mathrm{f}^2 - 145.121\,V_\mathrm{f}^3 & \text{if } V_\mathrm{f} < 0.3 \\ 1.5 + 5500\,V_\mathrm{f}^{18} & \text{if } V_\mathrm{f} \geq 0.3 \end{cases} \tag{12}$$

For usual volume fractions in unidirectional lamina, only the second of these expressions is applicable. Note that this expression reduces to $\xi \approx 1.5$ for $V_\mathrm{f} < 0.5$. This new value of $\xi = 1.5$ is proposed to compute E_2 through H-T equations, without compromising the advantages of these equations as far as simplicity is concerned.

6. Conclusions

The H-T equations are often used in the design practice because of their simplicity when compared to analytical approaches. However, the estimations for E_2 using these equations strongly depend on the value of the reinforcement parameter ξ which takes into account the geometry and spatial distribution of the reinforcement. It is common practice to use a value of $\xi = 2$ for calculation of E_2 using the H-T equations, despite this value was originally fitted to the solution for a square array provided by Adams and Doner. In this work, we have carried out finite element analyses taking into account a random distribution of the fibers and their diameters, which is

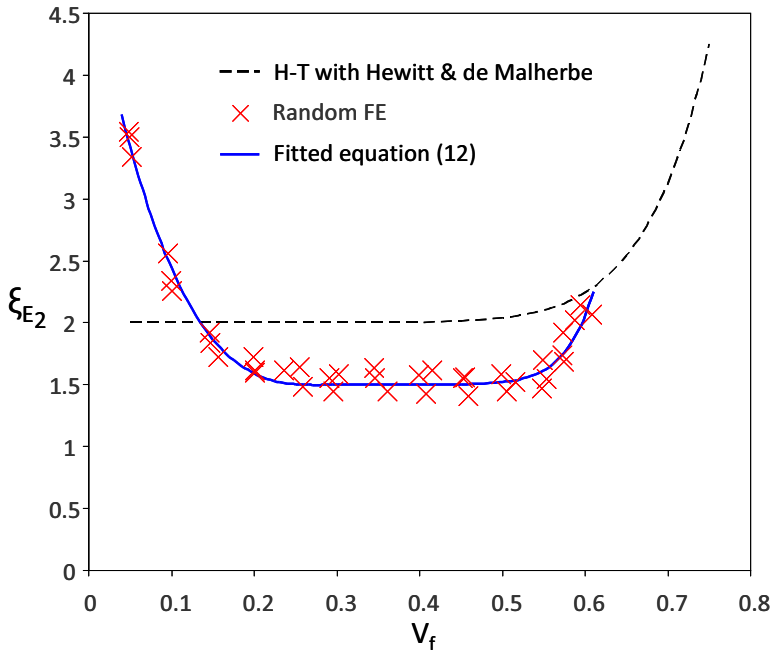

Figure 12: Plot of the expressions given in Eq. (12) fitted to the FE estimations of ξ with random distributions. Comparison with the Halpin-Tsai value ($\xi = 2$) modified with the Hewitt and de Malherbe approximation, Eq. (3).

more realistic that the theoretical square array distribution. The analysis procedure has been verified by first comparing the results for a square array distribution and several sensitivity analyses. As a result of the study, a new value of $\xi = 1.5$ has been proposed to compute E_2 through H-T equations in the range $V_\mathrm{f} \in [0.25, 0.55]$, under the assumption that a random distribution is more representative than the original square array distribution. Two analytical fitted expressions are also provided for a wider range of volume fractions.

Acknowledgements

The authors wish to thank the Ministerio de Economía y Competitividad for the support received in the framework of the project DPI2013-46641-R and the Generalitat Valenciana, Programme PROMETEO 2012/023. The authors also gratefully acknowledge the collaboration of Mr. Vicente Franco Parra.

References

[1] Halpin JC. Primer on Composite Materials Analysis. 2nd Ed. CRC Press, Taylor & Francis, Boca Ratón, Florida, 1992.

[2] Jones RM. Mechanics of Composite Materials. 2nd Ed. Taylor & Francis, Philadelphia, 1999.

[3] Hull D. An Introduction to Composite Materials. Cambridge University Press, Cambridge, 1981.

[4] Gibson RF. Principles of Composite Materials Mechanics. CRC Press, Taylor & Francis, Boca Ratón, Florida, 2007.

[5] Matthews FL, Rawlings RD. Composite Materials: Engineering and Science. Chapman & Hall, London, 1994.

[6] Halpin JC, Tsai SW. Effects of environmental factors on composite materials. AFML-TR 67-423, 1969.

[7] Hewitt RL, de Malherbe MC. An approximation for the longitudinal shear modulus of continuous fibre composites. J Compos Mat 1970;4:280–282.

[8] Spencer A. The transverse moduli of fibre-composite material. Compos Sci Technol 1996;27:93–109.